

ELECTROCHEMICAL OXIDATIONS OF 1,3-DIHYDRO-1,3-DIAZA-AZULANONES AND EFFECTS OF REACTION TEMPERATURE

Katsuhiko Saito,* Yosuke Ueda, Ayako Kawamura, Akiyoshi Kajita, Hiroyuki Ishiguro, Takayasu Ido, Katsuhiko Ono, and Yasutaka Awadu

Department of Applied Chemistry, Nagoya Institute of Technology, Gokiso-cho, Showa-ku, Nagoya, 466-8555, Japan

Abstract Electrochemical oxidations of 1-tosyl-3-aryl-1,3-dihydro-1,3-diazaazulanones at 0 °C afforded 3-aryl-6-tosyl-1,3-dihydro-1,3-diazaazulanones *via* migrations of the tosyl group. However, the same type of electrochemical oxidations at an elevated temperature (25 °C) gave another type of product, *i.e.*, double bond isomers, 1-tosyl-3-aryl-1,3-dihydro-1,3-diazaazulanones *via* 1,5-hydrogen migration, together with 3-aryl-6-tosyl-1,3-dihydro-1,3-diazaazulanones.

On account of the sp^2 hybridization of two nitrogen atoms and a carbonyl group in the five-membered ring moiety, the 1,2,3,3a-tetrahydrocyclohepta[*d*]imidazol-2-one (1,3-dihydro-1,3-diazaazulanone) system (**1**) is considered to have a 12π -electrons electron-poor cross conjugated system.¹ This system (**1**) also contains a cycloheptatriene (tropolidene) system, which is known to form a well stabilized 6π -electrons aromatic cation system, tropylium ion,² leaving a suitable anion group. These facts suggest that the system (**1**) has an ability to generate both cation and anion forms under the appropriate reaction conditions.

As a precursor of a member of nonbenzenoid aromatic compounds, the thermochemical behaviors of **1** have been researched extensively, but the number of the documents on the electrochemistry of **1** seems to be small.³

As a series of our research on the reactivities of **1**,⁴ we investigated the reactivities of **1** under the electrochemical conditions. Here the results will be discussed.

Figure 1 demonstrates the cyclic voltammograms of 1-tosyl-3-*p*-substituted phenyl-1,3-dihydro-1,3-diazaazulanones (**1a-d**), and Table 1 shows the redox potentials of **1**. The oxidation potentials of all of **1** are almost the same value, suggesting that the substituents on the phenyl group have almost no influence on the oxidation potentials.

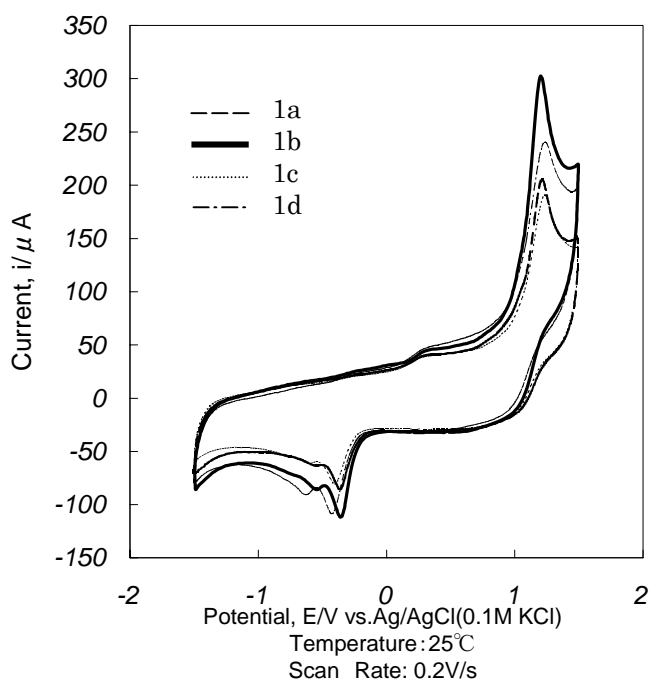
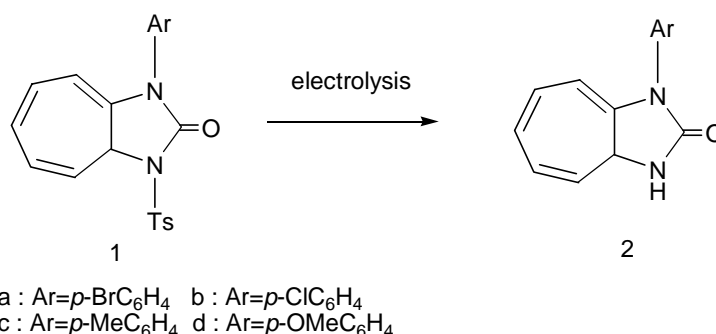


Table 1. Redox potentials of **1**.

Ar	Oxidation	Reduction
1a	1.24	-0.37
1b	1.23	-0.37
1c	1.19	-0.39
1d	1.21	-0.38

V vs. Ag/AgCl

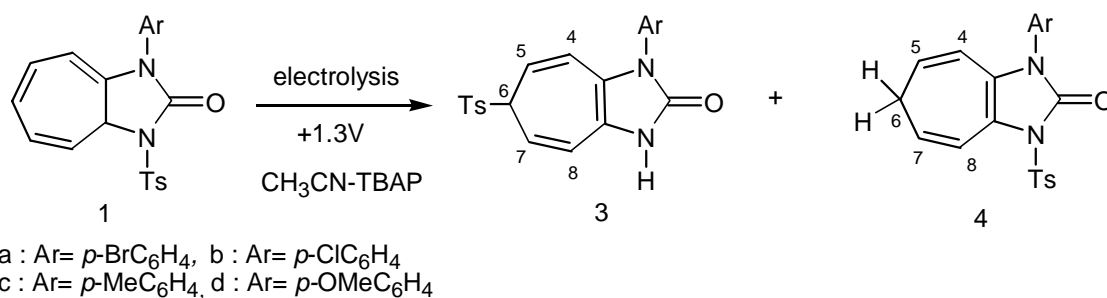
Figure 1. Cyclic voltammograms of **1**.



Previously we have reported that the electrochemical reduction of **1** afforded 3-aryl-1,3-dihydro-1,3-diazaazulane derivatives (**2**).⁵ This time we examined the electrochemical oxidation of **1**.

The electrochemical oxidations of **1** were influenced by both the substituents on the phenyl groups and the reaction temperatures. Preparative controlled-potential electrolysis of **1a** was performed in anhydrous acetonitrile containing tetra-*n*-butylammonium perchlorate (TBAP) as a supporting electrolyte. A platinum gauze was employed as an anode, and a platinum wire was employed as a cathode. Controlled-potential electrolysis was carried out at + 1.3 V vs. Ag/AgCl in a divided cell under a nitrogen stream at 0 °C. After evaporation of the solvent, the reaction mixture was chromatographed on silica gel column to give the products (**3**). As mentioned previously, the yields of **3a**, **3b**, **3c**, and **3d** were 20, 42, 50, and 37%, respectively.⁶

It was found that the yield of **3a** was improved by the reaction temperatures. Thus, the yield of **3a** increased to 37 % at 25 °C, and further to 79 % at 50 °C. However, at 70 °C, the yield slightly decreased to 64 %.

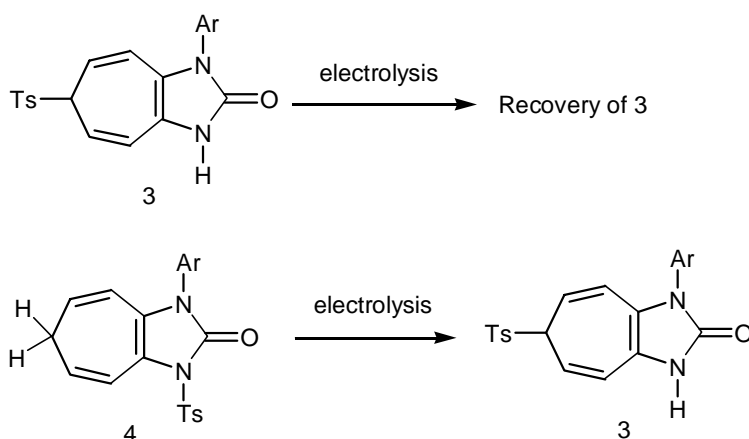


Another remarkable feature of this reaction is that the new products (**4**) were formed at only “medium” temperatures, *i.e.*, 25 and 50 °C. Thus the reaction of **1a** at 25 °C afforded a double bond isomer (**4a**) of **1a** in 8 % yield together with 37 % yield of **3a**. At higher temperature, **4a** was not obtained and only **3a** was formed as an isolatable product. As shown in Table 2, this aspect is observed in the reactions of all types of **1**.

Table 2. Effect of temperature on the product yields.

Starting materials	Temp (°C)	Yields (%)		
		3*	4*	Recovery of 1
1a	0	20	0	56
	25	37	8	19
	50	79	0	9
	70	64	0	0
1b	0	42	0	59
	25	51	9	26
	50	37	7	5
1c	0	50	0	67
	25	32	30	35
	50	24	0	18
	70	35	0	15
1d	25	37	12	20
	50	41	15	3

* Product yields were calculated except the recovery of **1**



The control experiments made it clear that **3** could be formed from **4**, but the inverse was not true. The electrochemical oxidations of **3** under the same reaction conditions as these of **1** resulted in the recoveries of the starting material (**3**). On the other hand, the oxidation of **4d** afforded **3d** in 14% yield.

The structure of **4** was determined using an X-Ray crystallographic analysis (Figure 2).⁷

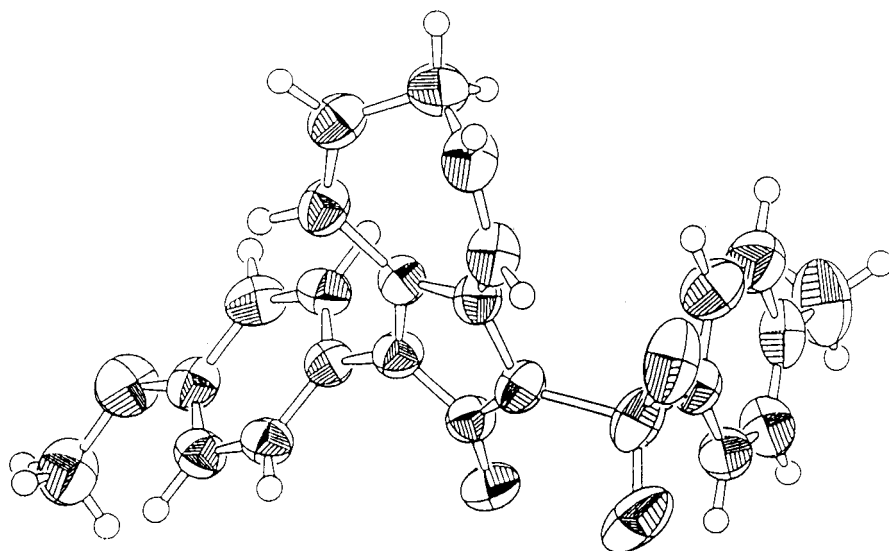


Figure 2. ORTEP drawing of **4**.

In order to investigate the possible influence of the temperature on the oxidation potential of **1**, the cyclic voltammetry of **1a** was measured at 0 and 25 °C. As clearly demonstrated in Figures 3 and 4, no influence was detected on the oxidation potential of **1a**.

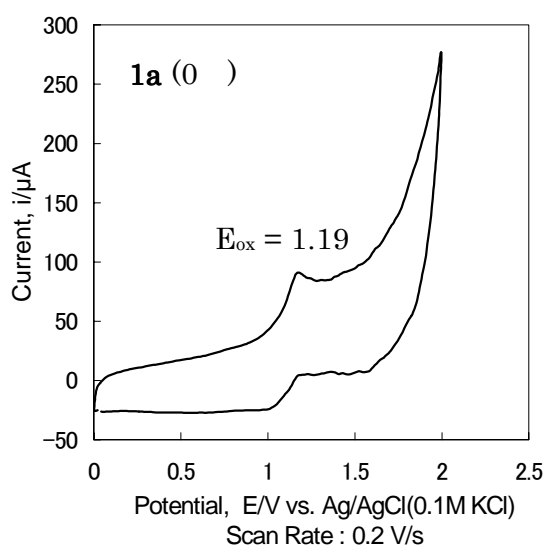


Figure 3.

Cyclic voltammograms of **1a** at 0 °C.

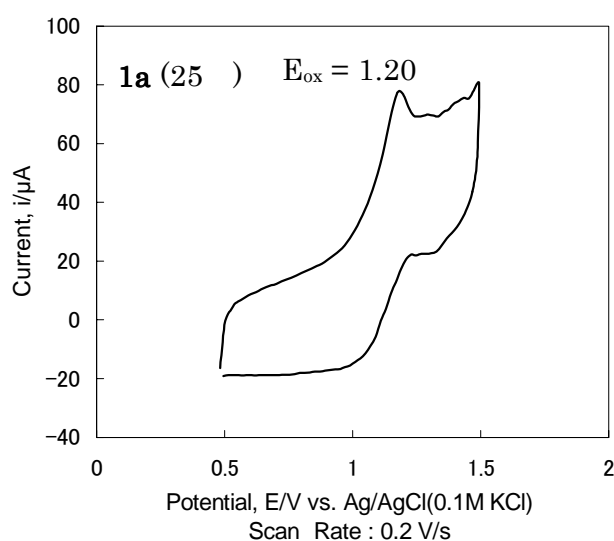
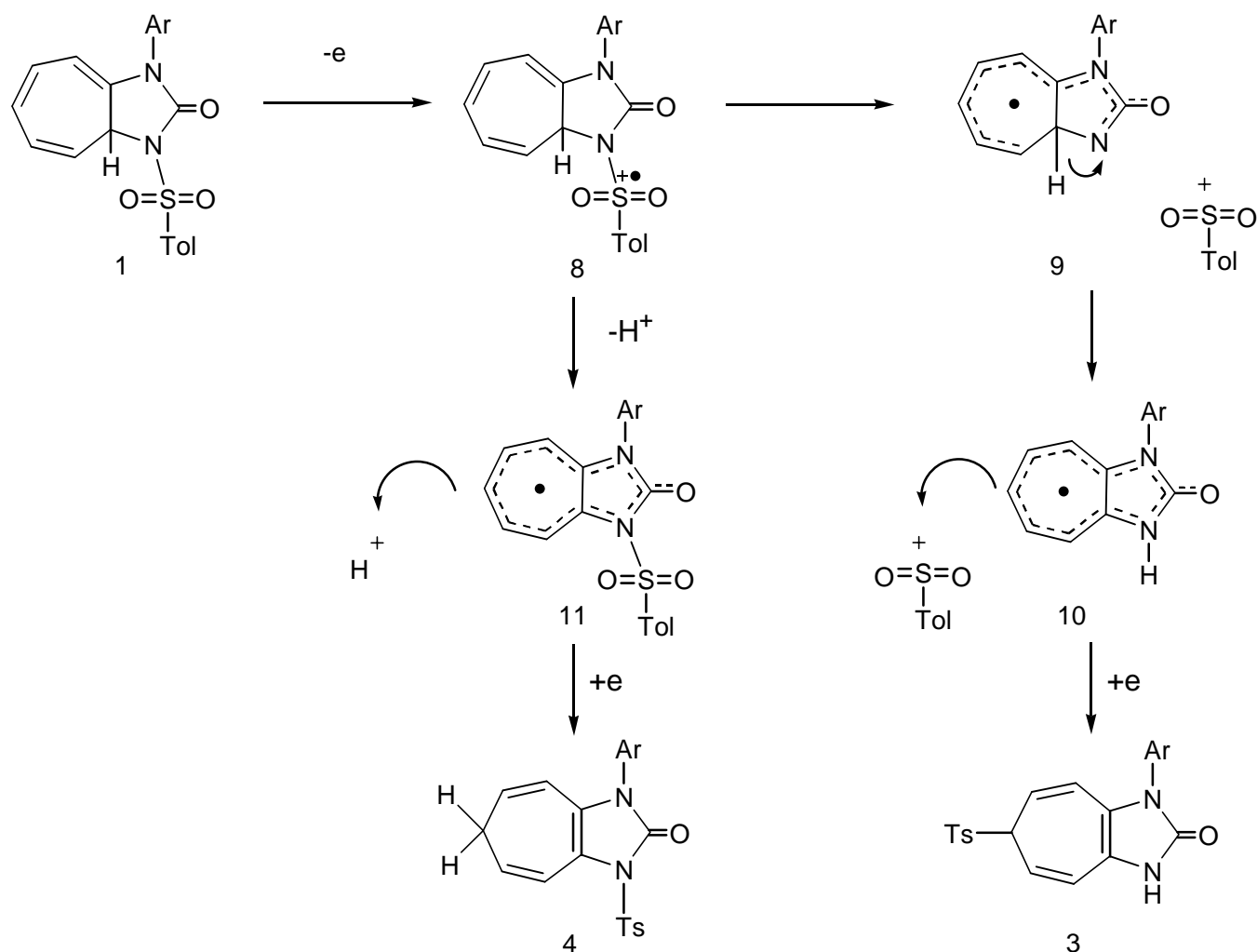


Figure 4.

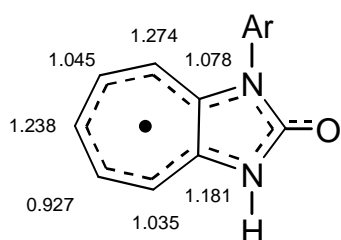
Cyclic voltammograms of **1a** at 25 °C.

These facts suggest that the temperature responsibility of the reaction is not the result of the electrochemical redox stage. The species generated by initial electron transfer from **1** should be always the same regardless of reaction temperature. The temperature should influence on the chemical process, which followed the electrochemical step.

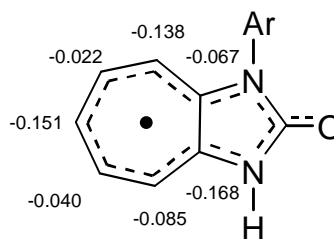


The electrochemical oxidation of **1** is considered to proceed as follows. As shown in Table 1, the oxidation potential of **1** is independent of the substituents on the phenyl groups. This fact suggests that the removal of the electron by the electrochemical oxidation process should not occur at the conjugated framework containing the phenyl group.

As a consequence, the electron on the tosyl group is considered to be removed to form a cation radical intermediate (**8**). The subsequent elimination of a tosyl cation generates a radical intermediate (**9**), which then affords a full conjugated cyclic radical intermediate (**10**) *via* a hydrogen migration. A recombination of the tosyl cation with **10** followed by an appropriate electron abstraction from the solvent or the cathode can afford the final product (**3**).



Free valences of **10**

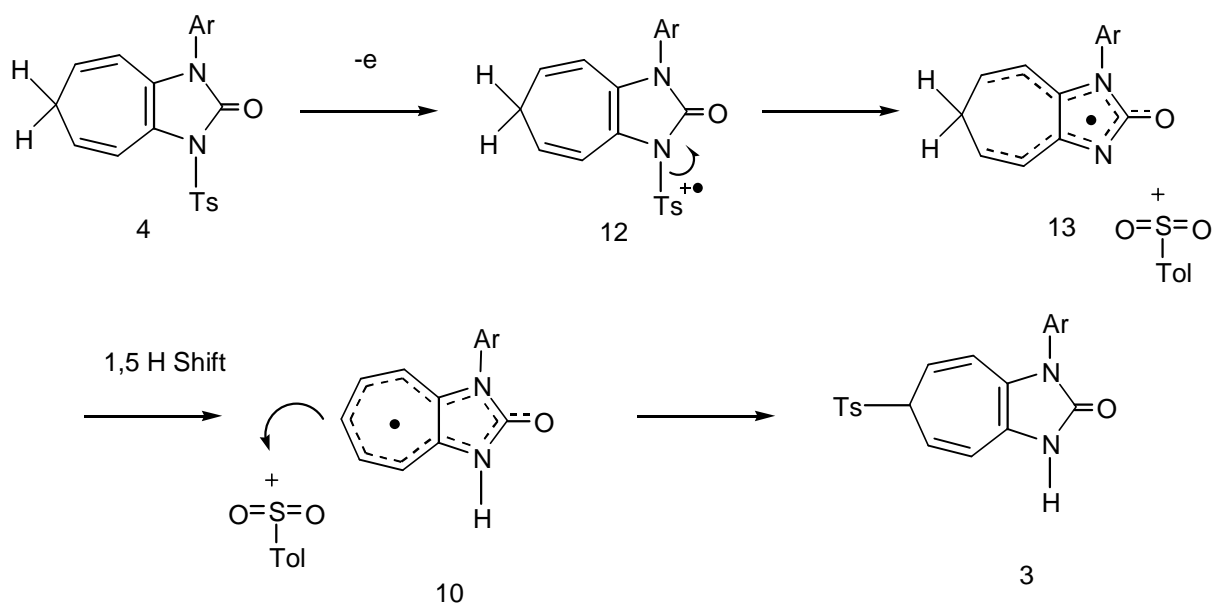


Electron densities of **10**

Figure 5.

Figure 5 demonstrates free valences and electron densities on the carbon atoms of **10**. The largest free valence (1.238) and the second largest electron density (-0.151) at the 6-position explain the position of the recombination of **10** and the tosyl cation.

The formation of **4** from **1** is also considered to proceed through the same cation radical intermediate (**8**) as the case of **3**. A 1,5-hydrogen migration via a full conjugated cyclic radical intermediate (**11**) can form the final product (**4**).



The electrochemical oxidation of **4** is thought to proceed as follows. One electron elimination from the tosyl group of **4** forms a cation radical intermediate (**12**), which then removes a tosyl cation to form a radical intermediate (**13**). A hydrogen migration on **13** to generate a stable full conjugated cyclic radical species generates a radical intermediate (**10**). The subsequent recombination between **10** and the tosyl cation followed by an appropriate electron abstraction affords the final product (**3**).

The mechanism of the influence of the reaction temperature on the reaction of **1** is not enough clear now. The authors suggest tentatively the following explanation.

A conceptual reaction coordinate is depicted in Figure 6. One electron oxidation of **1** generates a cation radical intermediate (**8**) via an appropriate transition state (**T**₁). Two reaction paths are possible for **8**, i.e., one is a path to **3** through a transition state **T**₂, and the other is to **4** through **T**₃. The activation energies for **T**₂ (**E**₂) and **T**₃ (**E**₃) are considered to control the choice of the reaction paths. At low temperature (0 °C) only the path to **3**, which requires a smaller activation energy is active. However, at elevated temperatures (25 or 50 °C) the second path, i.e., path to **4** becomes also active. But at the still higher temperatures (50 or 70 °C), the reactions of **4** are considered to take place. One of those may be the electrochemical oxidation to form **3**, and the other may be the decomposition of **4**.

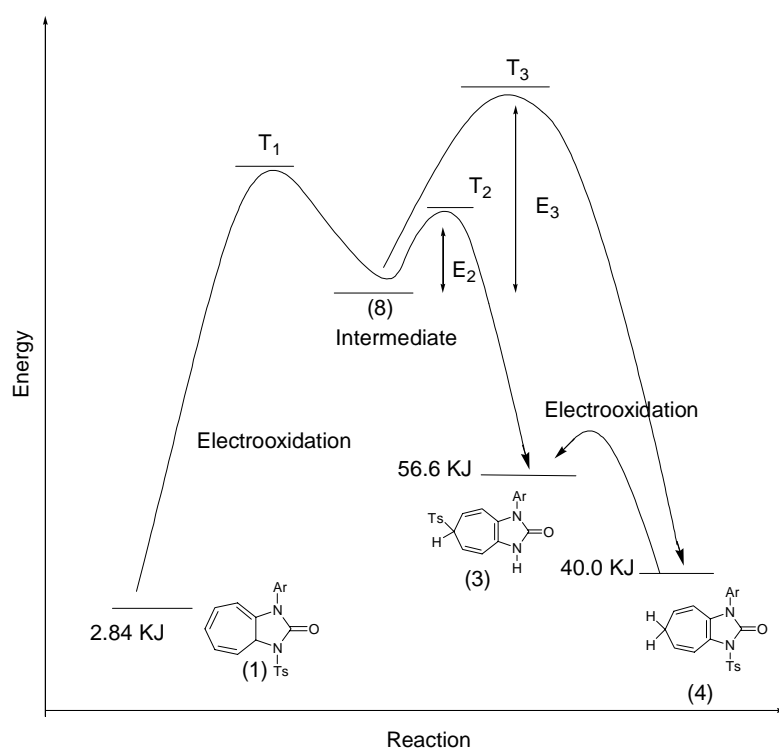


Figure 6. Effects of reaction temperature.

REFERENCES AND NOTES

1. W. E. Stewart and T. H. Siddall, *Chem. Rev.*, 1970, **70**, 517; T. Saito, Y. Fukazawa, Y. Fujise, and S. Ito, *Heterocycles*, 1977, **7**, 807.
2. T. Shono, T. Nozoe, H. Maekawa, Y. Yamaguchi, S. Kanetaka, T. Okada, and S. Kashimura, *Tetrahedron*, 1991, **47**, 593; K. Conrow, *J. Am. Chem. Soc.*, 1959, **81**, 5461; W. Tochtermann, C. Degel, H. O. Horstmann, and D. Krauss, *Tetrahedron Lett.*, 1970, 4719; W. D. Stohrer, *Chem. Ber.*, 1973, **106**, 970.

3. K. Takahashi, H. Yamamoto, and T. Nozoe, *Bull. Chem. Soc. Jpn.*, 1970, **43**, 2000; S. Kondo, H. Suzuki, T. Hattori, T. Ido, and K. Saito, *Heterocycles*, 1998, **48**, 1151; K. Saito, M. Hattori, T. Sato, and K. Takahashi, *ibid.*, 1992, **34**, 129.
4. T. Doi, H. Ishiguro, M. Sato, and K. Saito, *Heterocycles*, 1999, **51**, 1775; K. Saito, T. Ido, Y. Awadu, T. Kanie, and S. Kondo, *ibid.*, 2000, **53**, 519.
5. K. Ito, K. Saito, and K. Takahashi, *Bull. Chem. Soc. Jpn.*, 1992, **65**, 812; M. Nitta, H. Tomioka, A. Akaogi, K. Takahashi, K. Saito, and K. Ito, *J. Chem. Soc., Perkin Trans. 1*, **1994**, 2625; K. Sanechika, S. Kajigaeshi, and S. Kanemasa, *Chem. Lett.*, **1977**, 861.
6. T. Ido, S. Kondo, and K. Saito, *Heterocycles*, 1999, **50**, 63; K. Ito, K. Saito, and K. Takahashi, *ibid.*, 1991, **32**, 1117.
7. The MS, NMR, single crystal X-Ray analytical data of **4d** were as follows.

4d: Yellow crystals. mp 147 °. HRMS m/z: 408.1150. Calcd for C₂₂H₂₀N₂O₄S m/z: 408.1153. MS m/z (rel intensity): 408 (15, M⁺), 253 (100), 237 (5), 210 (8). IR (KBr): 1728, 1514, 1375, 1251, 1167 cm⁻¹. ¹H-NMR (CDCl₃), δ: 2.42 (3 H, s), 2.44 (2 H, t, H₆, *J* = 7.1 Hz), 3.84 (3 H, s), 5.26-5.42 (2 H, m, H₅, H₇), 6.05 (1 H, d, *J* = 9.3 Hz), 6.91 (2 H, d, *J* = 9.1 Hz), 7.08 (1 H, d, H₈, *J* = 9.8 Hz), 7.18 (2 H, d, *J* = 8.8 Hz), 7.31 (2 H, d, *J* = 8.5 Hz), 7.97 (2 H, d, *J* = 8.2 Hz). Crystal data: yellow prism, C₂₀H₂₀N₂O₄S, *M* = 408.47, monoclinic, space group *P*2₁/*a*, *a* = 15.511(3) Å, *b* = 6.402(1) Å, *c* = 19.969(4) Å, β = 91.672(5)°, *V* = 1982.0(6) Å³, *Z* = 4, *D*_{calcd} = 1.369 g/cm³, μ (MoKα) = 1.95 cm⁻¹, *F*(000) = 856.00. A Total of 5992 reflections for 2θ_{max} = 55° was collected with *I* > 2σ(*I*) using a Rigaku / MSC Mercury CCD diffractometer (MoKα radiation, λ = 0.71070 Å) at 296 K. The structure was solved using direct method (SHELXS-97) and refined by Full-matrix least squares analysis giving values of *R* = 0.102, *R*_w = 0.164, *R*₁ = 0.078, *S* = 1.44, ρ_{max} / ρ_{min} = 0.48 / -0.32 e⁻³.